

# Coherent responses of the resonance atom layer to short optical pulse excitation

Sergei O. Elyutin\*

*Department of Physics, Moscow Engineering Physics Institute, Moscow 115409, Russia*

(Received 12 September 2006; published 26 February 2007)

Coherent responses of resonance atom layer to short optical pulse excitation are numerically considered. The inhomogeneous broadening of one-photon transition, the local field effect, and the substrate dispersion are involved into analysis. For a certain intensity of incident pulses a strong coherent interaction in the form of sharp spikes of superradiation is observed in transmitted radiation. The Lorentz field correction and the substrate dispersion weaken the effect, providing additional spectral shifts. Specific features of photon echo in the form of multiple responses to a double or triple pulse excitation is discussed.

DOI: [10.1103/PhysRevA.75.023412](https://doi.org/10.1103/PhysRevA.75.023412)

PACS number(s): 42.50.Md, 51.70.+f, 78.20.Ci

## I. INTRODUCTION

There is a continuing broad interest in coherent transient processes in resonance media (see for example [1] and references therein). Among numerous papers in this field, the coherent transients in thin layers of polarizable matter hold separate position. In these structures the optically active excitations are represented by surface excitons [2,3]. Surface waves (surface polaritons) are characterized by some specific features in dispersion relations resulting from the reduced dimensionality of the medium. Exciton polaritons have been extensively studied in quantum wells [4–6] and thin films [7,8], thereupon the two-dimensional (2D) molecular systems such as the films of anthracene [9], the widely explored [10] aromatic molecular crystal, should be mentioned as a typical matter to observe exciton effects. The microcavities provide another example of artificial media where surface polaritons were investigated [11–13]. The generic feature of all mentioned systems is that they can be described in the frames of Bloch equations model, which is conventionally used to study the coherent processes in an ensemble of two-level atoms. For the weak light field the model reduces to the system of unharmonic oscillators generalizing the Lorenz model. A strong coupling between radiation and resonance matter demands to apply Bloch model in full [14]. A fundamental illustration for this was introduced in [8], where coherent effect of self-induced transparency of surface polaritons was predicted. The further development of that idea was reported in [15,16].

Refraction and reflection of ultrashort optical pulses at the interface of two dielectric media containing a thin layer of resonant systems (two-level systems [17], quantum wells [18–20],  $J$  aggregates [21]) is attributed by an account of dipole-dipole interaction [22,23] in microscopic field acting on resonance atoms.

The dynamics of pulsed radiation interaction with low-dimensional systems has been widely studied, for example in [24–30]. Thus, a specific spatial synchronism of photon echo generated by a thin resonance layer on an interface was considered in [29]. The transmission of ultrashort pulses through thin-film resonators filled with two-level resonance atoms

was discussed in [30]. The remarkable result in this field was the prediction of optical bistability [24,31–35] and the feasibility of the chaotic pulsation of the transmitted radiation [34]. The approaches worked out for conventional models were extended to another low dimension system, such as the layer of quantum dots [36], film of three level atoms [37,38], and another type of resonance, for instance, the two-photon resonance [39,40].

The purpose of this work is to demonstrate by numerical modeling, how a thin layer attributes, such as local field effect, a very small thickness of the film, the inhomogeneous broadening of resonance transition and even the dispersion of substrate material (Sec. I) can affect the transmittance of layer and the temporal shape of transmitted ultrashort pulses (Sec. II), including the observation of the photon echo effect [28,29,41,42] (Sec. III). It turned out that the Lorentz field correction plays an important role in film structures, causing spectral dynamical shifts of atomic system observable in strong coherent coupling of pulsed radiation with a film.

## II. A THIN FILM OF ATOMS ON AN INTERFACE

Let a thin film of atoms interacting resonantly with the electromagnetic field of light wave lie on the layer along the interface of two dielectric media in the  $X=0$  plane. The dielectric media surrounding the film are characterized by the dielectric permittivity  $\epsilon_a$  at  $x<0$  and  $\epsilon_b$  at  $x>0$ . Axis  $Z$  is chosen in the plane of the interface. The resonance atoms are described by a two-level model. The duration of the optical pulse is short in comparison with polarization and population difference relaxation times, but at the same time, it is much longer than an optical period. Therefore, the approximation of slowly varying complex amplitudes can still be applied. It is supposed that the thickness of the film  $l$  is of the order or less than the wavelength of resonant radiation  $l \sim \lambda$ .

Let the short pulse of the transversal electric (TE) wave be incident on the interface from the  $x<0$  side. The electric field vector  $\mathbf{E}$  of such wave is orthogonal to the  $ZX$  plane for all  $x$ , i.e., the polarization vectors of the incident, refracted, and reflected wave are collinear to the  $Y$  axis:  $\mathbf{E}=(0, E_y, 0)$ ,  $\mathbf{H}=(H_x, 0, H_z)$ . The reflected wave returns to the  $x<0$  half-space but the refracted wave propagates into the  $x>0$  half-space.

\*Email: address: soelyutin@email.mephi.ru

It is convenient to represent the field strength  $\mathbf{E}$ , and the polarization  $\mathbf{P}$  of the resonant atoms inside the film as

$$\mathbf{E}(x, z, t) = \int_{-\infty}^{\infty} \frac{d\omega d\beta}{2\pi 2\pi} \exp(-i\omega t + i\beta z) \tilde{\mathbf{E}}(x, \beta, \omega),$$

$$\mathbf{H}(x, z, t) = \int_{-\infty}^{\infty} \frac{d\omega d\beta}{2\pi 2\pi} \exp(-i\omega t + i\beta z) \tilde{\mathbf{H}}(x, \beta, \omega),$$

$$\mathbf{P}(z, t) = \int_{-\infty}^{\infty} \frac{d\omega d\beta}{2\pi 2\pi} \exp(-i\omega t + i\beta z) \tilde{\mathbf{P}}(\beta, \omega).$$

Outside the film the Fourier components  $\tilde{\mathbf{E}}(x, \beta, \omega)$  and  $\tilde{\mathbf{H}}(x, \beta, \omega)$  of the field vectors are determined by Maxwell's equations, and the components at  $x=0$  are determined by continuity condition so that for the TE case we obtain the system of equations

$$\frac{d^2 \tilde{E}}{dx^2} + (k^2 \varepsilon_j - \beta^2) \tilde{E} = 0, \quad \tilde{H}_x = -(\beta/k) \tilde{E}, \quad (1)$$

$$\tilde{H}_z = -\frac{i d\tilde{E}}{k dx}, \quad \tilde{E}_y = \tilde{E}$$

with the boundary conditions

$$\tilde{E}(x=0^-) = \tilde{E}(x=0^+),$$

$$\tilde{H}_z(x=0^+) - \tilde{H}_z(x=0^-) = 4\pi i k \tilde{P}_y(\beta, \omega).$$

Here  $j=1, 2$ ,  $k=\omega/c$ , and  $\beta$  is the propagation constant along the interface. Outside a thin film the solution of Eq. (1), with the allowance for the behavior of the field far from the film, has the form

$$\tilde{E}(x, \beta, \omega) = \begin{cases} \tilde{E}_{in} \exp(iq_1 x) + \tilde{E}_{ref} \exp(-iq_1 x), & x < 0 \\ \tilde{E}_{tr} \exp(iq_2 x), & x > 0, \end{cases} \quad (2)$$

where  $q_j = \sqrt{k^2 \varepsilon_j - \beta^2}$ ,  $j=a, b$ .

The boundary conditions at  $x=0$  provide the relations between the amplitudes of the incident  $\tilde{E}_{in}$ , reflected  $\tilde{E}_{ref}$ , and refracted (transmitted)  $\tilde{E}_{tr}$  waves and the surface polarization  $\tilde{P}_S = \tilde{P}_y$  of the film

$$\begin{aligned} \tilde{E}_{tr}(\beta, \omega) &= \frac{2q_a}{q_a + q_b} \tilde{E}_{in}(\beta, \omega) + i \frac{4\pi k^2}{q_a + q_b} \tilde{P}_S(\beta, \omega) \\ \tilde{E}_r(\beta, \omega) &= \frac{q_a - q_b}{q_a + q_b} \tilde{E}_{in}(\beta, \omega) + i \frac{4\pi k^2}{q_a + q_b} \tilde{P}_S(\beta, \omega). \end{aligned} \quad (3)$$

It is convenient to introduce the notations for the Fresnel transmission coefficient  $T_{TE}$  and the coupling constant  $\kappa_{TE}$

$$T_{TE}(\beta, \omega) = \frac{2q_1}{q_1 + q_2}, \quad \kappa_{TE}(\beta, \omega) = \frac{4\pi k^2}{q_1 + q_2}.$$

For the given polarization of the film, relations (3) determine the field in the entire space. It should be emphasized that (3) in no way are related with the assumption of slowly varying envelopes of the optical pulses and are exact.

We shall now focus our attention on the refracted wave. Let us consider only the case  $\varepsilon_a < \varepsilon_b$ , where the total internal reflection does not occur for any angle of incidence  $\varphi = \arccos(q_a/k\sqrt{\varepsilon_a})$ , and Snell's law sets the refraction angle  $\psi$

$$\sin \psi = (\beta/k\sqrt{\varepsilon_b}) = \sqrt{\varepsilon_a/\varepsilon_b} \sin \varphi. \quad (4)$$

We concentrate on the case of (TE) waves. The Fourier components of the amplitudes of the macroscopic fields are coupled by Eq. (3), providing an exact relationship

$$\tilde{E}_{tr}(\beta, \omega) = T(\beta, \omega) \tilde{E}_{in}(\beta, \omega) + i\kappa(\beta, \omega) \tilde{P}_S(\beta, \omega). \quad (5)$$

Indices TE are omitted for brevity.

The surface polarization  $\tilde{P}_S(\beta, \omega)$  is determined by the thin layer atom response. It is generated by the local field  $\tilde{E}_L(\beta, \omega)$ , which, in its turn, is the sum of the field in the film  $\tilde{E}_{tr}(\beta, \omega)$  and the bulk polarization  $\tilde{P}(\beta, \omega)$  [24,31]

$$\tilde{E}_L(\beta, \omega) = \tilde{E}_{tr}(\beta, \omega) + 4\pi\alpha \tilde{P}(\beta, \omega). \quad (6)$$

Parameter  $\alpha$  accounts the effect of environment,  $\alpha=1/3$  for isotropic distribution of atoms in bulk material.

An optical pulse incident on the film presents in the form of a quasiharmonic wave

$$E(x, z, t) = \mathbf{E}(x, z, t) \exp[-i\omega_0 t + i\beta_0 z],$$

where  $\mathbf{E}(x, z, t)$  is the pulse envelope varying slowly in space and in time,  $\beta_0 = \beta(\omega = \omega_0)$  is the propagation constant at the frequency of the pumping wave.

The condition of the quasiharmonicity can be expressed in terms of Fourier components of electric field  $\tilde{E}(\omega, \beta)$  the pulse and its shape  $\mathbf{E}(\omega, \beta)$ . This condition writes as

$$\tilde{E}(\omega_0 + \omega, \beta_0 + \beta) = \mathbf{E}(\omega, \beta)$$

with  $\omega \ll \omega_0$  and  $\beta \ll \beta_0$

Thus, under the approximation of quasiharmonic waves the coupling equations (3) is rewritten as

$$\begin{aligned} \mathbf{E}_{tr}(\beta, \omega) &= T(\beta_0 + \beta, \omega_0 + \omega) \mathbf{E}_{in}(\beta, \omega) + i\kappa(\beta_0 + \beta, \omega_0 + \omega) \\ &\quad \times \mathbf{P}_S(\beta, \omega), \end{aligned} \quad (7a)$$

$$\begin{aligned} \mathbf{E}_r(\beta, \omega) &= R(\beta_0 + \beta, \omega_0 + \omega) \mathbf{E}_{in}(\beta, \omega) + i\kappa(\beta_0 + \beta, \omega_0 + \omega) \\ &\quad \times \mathbf{P}_S(\beta, \omega). \end{aligned} \quad (7b)$$

In (7) the Fourier component of the slowly varying surface polarization  $\mathbf{P}_S(\beta, \omega)$  is the functional of the Fourier component of the local field envelope  $\mathbf{E}_L(\beta, \omega)$

$$\mathbf{E}_L(\beta, \omega) = \mathbf{E}_{tr}(\beta, \omega) + 4\pi\alpha \mathbf{P}(\beta, \omega). \quad (8)$$

Here  $\mathbf{P}(\beta, \omega)$  is the Fourier component of the bulk polarization of the film material.

In order to take into account the finite spectral width of the wave packet, which formed a quasiharmonic signal, one can expand the coefficients  $T(\beta_0 + \beta, \omega_0 + \omega)$ ,  $R(\beta_0 + \beta, \omega_0 + \omega)$

+ $\omega$ ), and  $\kappa(\beta_0 + \beta, \omega_0 + \omega)$  in a power series of  $\omega$  until several first terms of these series.

For the sake of simplicity let us assume that the incident wave is isotropic in the plane of interface, so the terms proportional to  $\beta/\beta_0$  in the expansion of  $T$ ,  $R$ , and  $\kappa$  are ignored.

Then one can write with the accuracy up to the second power of  $\omega$

$$T(\beta_0 + \beta, \omega_0 + \omega) \approx T(\beta_0, \omega_0) + T_1(\beta_0, \omega_0)\omega + T_2(\beta_0, \omega_0)\omega^2,$$

$$R(\beta_0 + \beta, \omega_0 + \omega) \approx R(\beta_0, \omega_0) + R_1(\beta_0, \omega_0)\omega + R_2(\beta_0, \omega_0)\omega^2.$$

Only the first term of a corresponding series is kept for the coupling constant, i.e.,  $\kappa(\beta_0 + \beta, \omega_0 + \omega) \approx \kappa(\beta_0, \omega_0)$ .

With this account, the coupling equations (7) allow us to transfer from spectral presentation to dynamic presentation

$$\mathbf{E}_{tr}(z, t) = \left( T_0 + iT_1 \frac{\partial}{\partial t} - T_2 \frac{\partial^2}{\partial t^2} \right) \mathbf{E}_{in}(z, t) + i\kappa \mathbf{P}_S(z, t), \quad (9a)$$

$$\mathbf{E}_r(z, t) = \left( R_0 + iR_1 \frac{\partial}{\partial t} - R_2 \frac{\partial^2}{\partial t^2} \right) \mathbf{E}_{in}(z, t) + i\kappa \mathbf{P}_S(z, t). \quad (9b)$$

The notations introduced in (9) are

$$T_0 = \frac{2 \cos \varphi}{\cos \varphi + \sqrt{\cos^2 \varphi + (\varepsilon_b - \varepsilon_a)/\varepsilon_a}} \quad (10)$$

$$\kappa = \frac{4\pi(\omega/c)}{\cos \varphi + \sqrt{\cos^2 \varphi + (\varepsilon_b - \varepsilon_a)/\varepsilon_a}}.$$

Let atoms or molecules, whose resonance levels are coupled by one photon transition at the frequency of pulse carrier, form a thin layer.

The slow varying matrix elements of density matrix satisfy Bloch equations

$$\frac{\partial \sigma_{\Delta\omega}}{\partial t} = i\Delta\omega \sigma_{\Delta\omega} + i\Omega n_{\Delta\omega}, \quad \frac{\partial n_{\Delta\omega}}{\partial t} = \frac{i}{2}(\sigma_{\Delta\omega} \Omega^* - \sigma_{\Delta\omega}^* \Omega),$$

where  $\Omega = d\mathbf{E}_L/\hbar$  is an instant Rabi frequency,  $d$  is a matrix element of the operator of dipole moment of resonance transition. The variables  $n_{\Delta\omega}$  and  $\sigma_{\Delta\omega}$ , depending on the detuning  $\Delta\omega$ , are related to the matrix elements of the density matrix by the relationships  $n = \rho_{11} - \rho_{22}$ ,  $\rho_{12} = \sigma \exp(-i\omega_0 t + i\beta_0 z)$ .

The surface polarization  $\mathbf{P}_S(z, t)$  expresses in terms of these quantities as

$$\mathbf{P}_S(z, t) = dn_a l \langle \sigma_{\Delta\omega}(z, t) \rangle,$$

where  $n_a$  is the bulk density of resonance atoms, the angular brackets means a summation over the frequency detuning  $\Delta\omega$  of resonance frequency of individual atoms from the center of the inhomogeneous line. Referring to Eqs. (8) and (9), formulas (10) and the relationship

$$\mathbf{P}(z, t) = dn_a \langle \sigma_{\Delta\omega}(z, t) \rangle,$$

the instant Rabi frequency is written in the following form:

$$\Omega = \frac{4\pi n_a d^2}{\hbar} \left( \alpha + i \frac{\kappa l}{4\pi} \right) \langle \sigma_{\Delta\omega} \rangle + \left( T_0 + iT_1 \frac{\partial}{\partial t} - T_2 \frac{\partial^2}{\partial t^2} \right) \times \frac{d}{\hbar} \mathbf{E}_{in}(z, t).$$

Following [24,25], the ‘‘cooperative time’’  $t_c = \hbar(4\pi n_a d^2)^{-1}$  can serve as the time scale of the problem. Then the main equations of the model write

$$\frac{\partial \sigma_\nu}{\partial \tau} = i\gamma \nu \sigma_\nu + i e_{loc} n_\nu, \quad \frac{\partial n_\nu}{\partial \tau} = \frac{i}{2}(\sigma_\nu e_{loc}^* - \sigma_\nu^* e_{loc}), \quad (11a)$$

$$e_{loc} = f(\tau) + (\alpha + ig\chi) \langle \sigma_\nu \rangle, \quad (11b)$$

where  $\nu = \Delta\omega T_2^*$ ,  $\gamma = t_c / T_2^*$ ,  $\chi(\varphi) = 2\pi[\sqrt{\varepsilon_a} \cos \varphi + \sqrt{\varepsilon_a \cos^2 \varphi + (\varepsilon_b - \varepsilon_a)}]^{-1}$ ,  $\tau = t/t_c$ , thickness factor  $g = l/\lambda$ ,  $\lambda$  is the wavelength of the carrier wave,  $e_{loc(in)} = dE_{loc(in)}\hbar^{-1}t_c$ ,  $T_2^*$  is the inhomogeneous dephasing time,  $\langle \dots \rangle$  means averaging over the radiators  $\nu$  within the inhomogeneous resonance absorption line, and the field penetrated the layer is

$$f(\tau) = \left( T_0 + iT_1 \frac{\partial}{\partial \tau} - T_2 \frac{\partial^2}{\partial \tau^2} \right) e_{in},$$

$$T_0 = T_0, \quad T_1 = T_1/t_c, \quad T_2 = T_2/t_c^2.$$

The macroscopic field

$$e_{tr} = f(\tau) + ig\chi \langle \sigma_x \rangle \quad (12)$$

is a detectable field spreading beyond the interface.

The characteristic for the two-level systems cooperative time  $t_c = \hbar(4\pi n_a d^2)^{-1}$  is the time the polarization is induced by the field of the traveling pulse. If to choose the dipole moment  $d \sim 10^{-18}$  CGSE and the density of resonance atoms  $n_a \sim 10^{18}$  cm $^{-3}$ , then  $t_c \approx 8 \cdot 10^{-11}$  s. The characteristic field strength can be determined from the condition  $d\mathbf{E}_{char}\hbar^{-1}t_c \approx 1$ .  $\mathbf{E}_{char} = 4\pi n_a d = \hbar(dt_c)^{-1} \approx 10$  CGSE. For comparison, the intra-atomic field can be estimated as  $\mathbf{E}_{atom} \approx 10^6$  CGSE. The corresponding peak intensity of the pulses, illuminating the film, is  $I_{char} = c\mathbf{E}^2/8\pi \approx 10^4$  W cm $^{-2}$ . The Lorentz correction provides  $\mathbf{E}_{Lr} = 4\pi n_a \alpha d = \alpha \mathbf{E}_{char} \approx 3$  CGSE. The strength of the field of radiation from the atom layer is  $\mathbf{E}_{rad} = (4\pi)^{-1} \kappa l \cdot \hbar(dt_c)^{-1} = \sqrt{\varepsilon_a} \chi g \mathbf{E}_{char} \approx 20-30$  CGSE.

A thin film [21] of  $J$ -aggregated cyanine dye molecules [43] with the thickness of about resonance radiation wavelength could serve as an example of realistic 2D system that matches the above estimates regarding the important super-radiant damping constant  $t_c^{-1}$  taken with slightly lower bulk density of molecules ( $\sim 10^{17}$  cm $^{-3}$ ) or smaller dipole moment  $d$  than in [21].

So the field equation (11b) is rewritten in a straightforward form ( $\varepsilon_a = 1$ )

$$e_{loc} = \left( T_0 + iT_1 \frac{\partial}{\partial \tau} - T_2 \frac{\partial^2}{\partial \tau^2} \right) e_{in} + (e_{Lr} + ie_{rad}) \langle \sigma_\nu \rangle, \quad (13)$$

where  $e_{Lr(rad)} = \mathbf{E}_{Lr(rad)}/\mathbf{E}_{char}$ .

The dispersion coefficients  $T_1$  and  $T_2$  in the combined transmittivity can be estimated by the inequalities  $T_1/\tau_p < T_0$ ,  $T_2/\tau_p^2 < T_0$ , where  $\tau_p$  is the dimensionless duration of an excitation pulse. As the Fresnel coefficient  $T_0 \approx 1$ , then for the pulses of several units in duration the values of  $T_1$  and  $T_2$  can be relatively large and be both positive and negative sign.

### III. OPTICAL PULSE TRANSMISSION THROUGH A THIN FILM OF RESONANCE ATOMS

In the subsequent calculations the pulse incident film are assumed having either the sech form:  $e_m \operatorname{sech}[(\tau - \tau_0)\tau_p^{-1}]$  or in the form of smooth step

$$\frac{e_m}{2} \{ \tanh[(\tau - \tau_0)\tau_f^{-1}] - \tanh[(\tau - \tau_0 - \tau_p)\tau_f^{-1}] \},$$

where  $\tau_0$ ,  $\tau_p$ , and  $\tau_f$  are the pulse delay, pulse duration, and pulse edge duration time, respectively.

In this section, the resonance absorption line is supposed to be narrow and  $\delta$  represents a certain detuning from exact resonance. Then Eq. (11) can be rewritten as

$$\frac{\partial \sigma}{\partial \tau} = i(\delta + \alpha n)\sigma + i n e_{ir}, \quad \frac{\partial n}{\partial \tau} = \frac{i}{2}(e_{ir}^* \sigma - \sigma^* e_{ir}), \quad (14)$$

$$e_{ir} = f(\tau) + i g \chi \sigma, \quad \gamma \nu = \delta.$$

#### A. Pulse shape

To obtain simple formulas let the Lorentz field effect be absent  $\alpha = 0$ . Then, equations of the model (11) at exact resonance ( $\delta = 0$ ) yields the solution

$$\sigma = i \sin \Theta, \quad n = \cos \Theta, \quad \Theta = \int_0^\tau e_{ir}(\tau') d\tau'.$$

In terms of Bloch angle  $\Theta$  the coupling equation (11b) or (13) transform to

$$\frac{\partial \Theta}{\partial \tau} + e_{rad} \sin \Theta = T_0 e_{in}(\tau). \quad (15)$$

The solution of (15) was found in [27] for a rectangular pulse form. In the case  $e_m \ll 1$  the field of the transmitted pulse looks like

$$e_{tr} = \begin{cases} -T_0 e_m [\exp(e_{rad} \tau) - 1] \exp(-e_{rad} \tau), & \tau > \tau_p \\ T_0 e_m \exp(-e_{rad} \tau), & 0 \leq \tau \leq \tau_p. \end{cases} \quad (16)$$

To illustrate this, the variant of numerical simulation of (11) for a smooth step input pulse is depicted in Fig. 1(a). We neglect the substrate dispersion at this stage. It is seen that the weak pulse is almost totally reflected. If the amplitude of the exciting field is not too large, than the field is in resonance with the quantum system and so the pulse is strongly reflected from the layer as it was discussed in a number of papers [24,25,31]. The exponential tails at the leading and

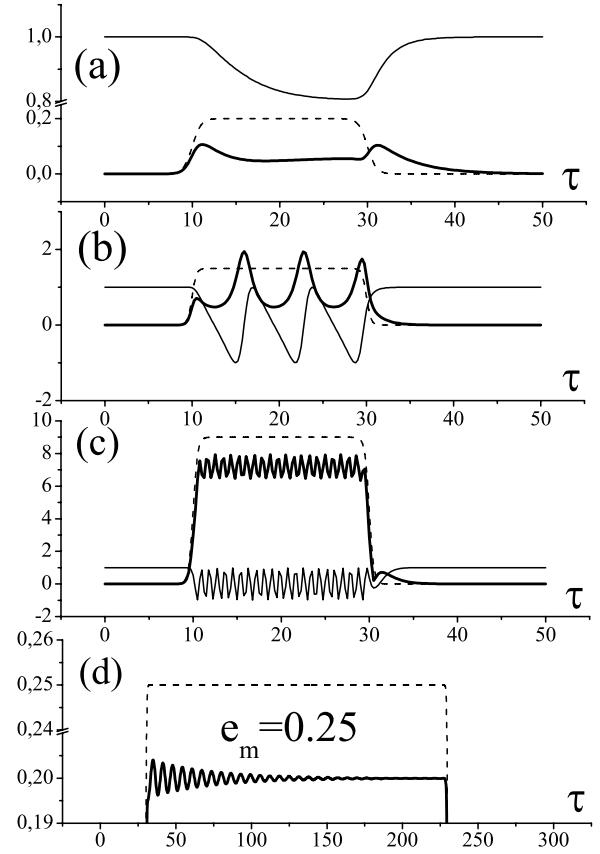


FIG. 1. The transmitted pulse envelope  $|e_{tr}(\tau)|$  (thick solid curve) and population difference  $n(\tau)$  (thin solid curve) under excitation by plateau pulses  $e_{in}(\tau)$  (dash curve) for Lorentz parameter  $\alpha$  and the thickness factor  $g$  values correspondingly: 0.1 and 0.1 (a), 0.3 and 0.3 (b), 1.0 and 0.3 (c), 1.0 and 0.01 (c). Exact resonance  $\delta = 0$ . All variables are dimensionless (see the text).

the trailing edge of the pulse are the signals of free induction decay. The calculation run with the Lorentz factor  $\alpha \approx 1$  revealed the role of the local field [22] as the additional detuning causing the shift from resonance and the loss of coherency. That leads to practically total transparency of the film for pulse radiation [Fig. 1(a)].

In the intermediate case,  $T_0 e_m \ll 1$  the solution of equations (14) in the interval  $0 \leq \tau \leq \tau_p$  contains characteristic hyperbolic functions [4]

$$e_{tr}(\tau) = T_0 e_m Q_1^2 [Q_1 \sinh(e_{rad} Q_1 \tau) + \cosh(e_{rad} Q_1 \tau) - T_0^2 e_m^2]^{-1},$$

where  $Q_1^2 = 1 - T_0^2 e_m^2$ .

The step pulse [Fig. 1(b)] splits into a series of spikes whose number, similar to the self-induced transparency (SIT) [44] phenomenon, grows with the increase of  $\Theta(\tau_p)$ . The spikes on the profile of the transmitted signal are the pulses of superradiation arose due to the pendulum motion of the Bloch vector. The pendulum quickly passes the point of equilibrium while it moves slowly near nonequilibrium position. In Fig. 1(b), the population of the ground level exhibits Rabi oscillation. That means that the Bloch vector makes the full rotation so that the population restores to the beginning of the next peak. We observe a SIT-like splitting of the power-

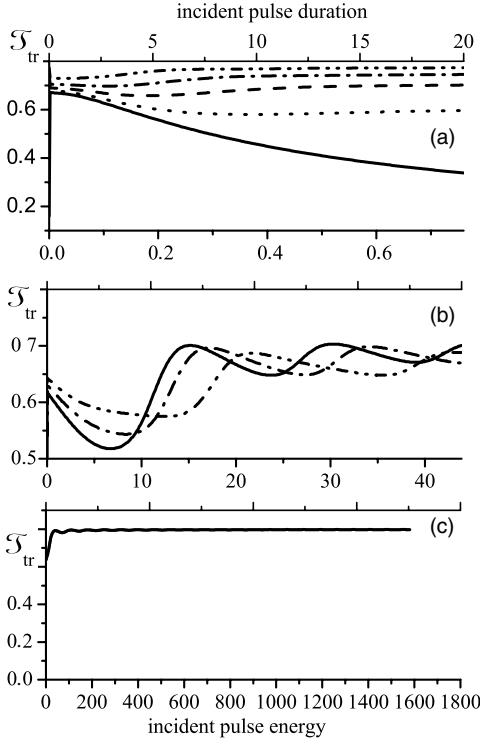


FIG. 2. Transmission coefficient vs incident pulse energy for weak (a), medium (b), and strong (c) input fields. (a) factor  $g=0.1$ , parameter  $\alpha$  values: solid curve  $-0.0$ , dot curve  $-0.3$ , dash curve  $-0.5$ , dash-dot curve  $-0.7$ , dash-dot-dot curve  $-1.0$ . (b)  $g=0.3$ , solid  $-0.0$ , dash-dot  $-0.7$ , dash-dot-dot  $-1.0$ . (c)  $g=0.3$ , same curve for any  $\alpha$  from the above set. Exact resonance  $\chi=0$ . All variables are dimensionless.

ful incident pulse into several subpulses of superradiation with a corresponding oscillation of population.

At last, for the strong fields, when  $T_0 e_m > 1$  at time interval  $0 \leq \tau \leq \tau_p$  the corresponded solution of the reduced problem (14) has the oscillatory form [Fig. 1(c)]

$$e_{tr}(\tau) = T_0 e_m Q_2^2 [T_0^2 e_m^2 + Q_2 \sin(e_{rad} Q_2 \tau) - \cos(e_{rad} Q_2 \tau)]^{-1},$$

where  $Q_2^2 = T_0^2 e_m^2 - 1$

All three cases are common in that the dynamics of transmission of short pulses is determined by parameter  $e_{rad}$ , responsible for effectiveness of radiation interaction with the layer of resonance atoms. It is interesting that in the case of weak interaction [Fig. 1(d)] the quasicontinuous excitation causes the response in the form of damping oscillations tending to a stationary value [37], but only when the reaction of the film is weak ( $g < 1$ ).

### B. Transmission coefficient

If we were to introduce the transmission coefficient as a square root of the ratio of the transmitted pulse energy to the incident pulse energy then the transmission coefficient for the weak rectangular pulses can be derived after some algebra from (16)

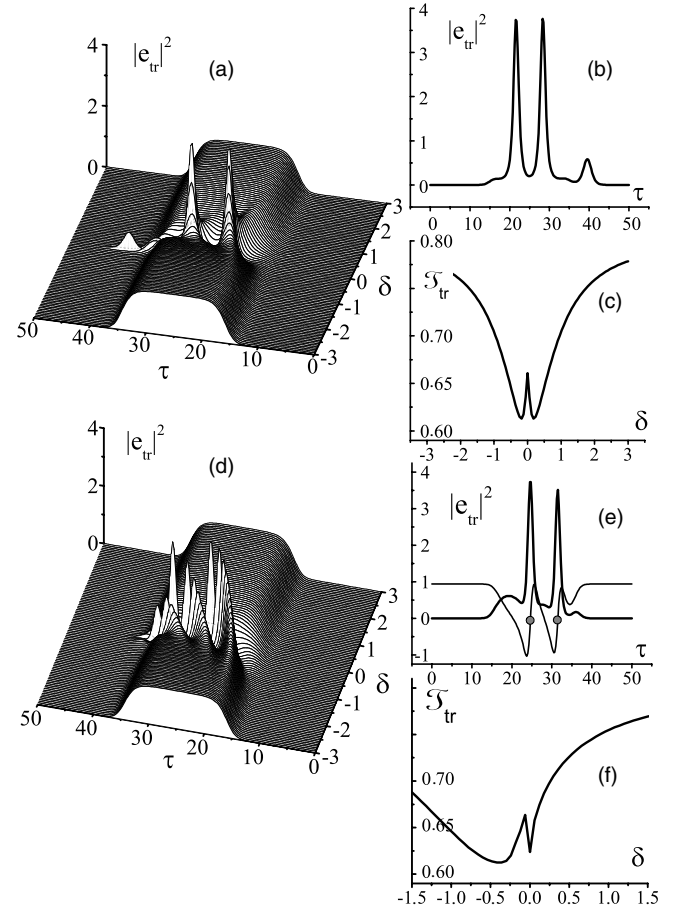


FIG. 3. The profile of transmitted intensity for a pulse of medium height under the sweep of detuning  $\delta$ .  $T_1=0$ ,  $T_2=0$ . (a)  $\alpha=0$ ; (b)  $\alpha=0$ ,  $\delta=0$ ; (c)  $\alpha=0$ ; (d)  $\alpha=1$ ; (e) transmitted pulse envelope (thick solid curve), total detuning  $\delta_{tot}(\tau) = \delta + \alpha n(\tau)$  (thin solid curve),  $\alpha=1$ ,  $\delta=0$ ; (f)  $\alpha=1$ . All variables are dimensionless.

$$T_{tr} = T_0 \tau_p^{-1/2} [1 - \exp(-\tau_p)]^{1/2}. \quad (17)$$

Expression (17) gives  $T_{tr} = T_0(1 - \tau_p/2)^{1/2}$  for  $\tau_p \ll 1$ , and  $T_{tr} = T_0 \tau_p^{-1/2}$  for  $\tau_p \gg 1$ . That means that a film of resonance atoms serves as a mirror for the long weak pulses.

In other cases the numerical analysis seemed to be more adequate. Each point on graphics (Fig. 2) is the result of the solution of the whole system (11) with a subsequent integration of the solution over time. The pulse shapes for the final pulse duration for each of three incoming amplitude in Figs. 2(a)–2(c) are depicted on the corresponding panels in Fig. 1.

In Fig. 2(a) the graphic is placed in the transmission coefficient  $T_{tr}$  vs incident pulse energy at the constant pulse amplitude  $e_{in}=0.2$ . The solid curve exhibits the anticipated reflection of a weak pulse (17). The transient regime ( $e_m = 1.5$ ) is featured by the oscillation of the transmittivity [Fig. 2(b)] due to the arising of new peaks on the temporal profile of a transmitted pulse [Fig. 1(b)]. The transparency of the resonance atom layer reaches the Fresnel limit  $T_0$  [Fig. 2(c)] and it does not practically alter with the energy growth when the amplitude of the input pulses is sufficiently large [Fig. 1(c)].

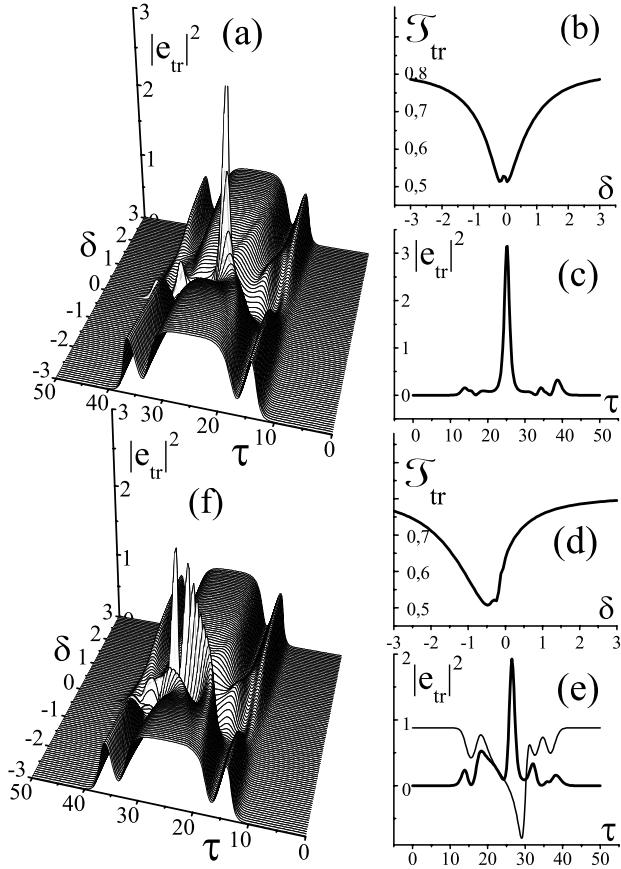


FIG. 4. The profile of transmitted intensity for a pulse of medium height under the sweep of detuning  $\delta$ . Effect of substrate dispersion is included ( $T_1=2$ ,  $T_2=-4$ ) in compare with calculation in Fig. 3. (a)  $\alpha=0$ , (b)  $\alpha=0$ , (c) transmitted intensity envelope at  $\alpha=0$ ,  $\delta=0$ ; (d)  $\alpha=1$ , (f)  $\alpha=1$ , (e) transmitted intensity envelope (thick solid curve), total detuning  $\delta_{tot}(\tau)=\delta+an(\tau)$  (thin solid curve),  $\alpha=1$ ,  $\delta=-0.2$ . All variables are dimensionless.

### C. Local field effect in coherent transmission

Lorentz field contribution does have a noticeable effect only for weak and intermediate pulse amplitudes when the action of the external field and the Lorentz field correction can be compared. Then the presence of the local field is accounted as an additional detuning, which drives the quantum system out from resonance. For a strong pulse excitation, the contribution of the local field effect is negligible [Fig. 1(c)].

The three-dimensional (3D) plot in Fig. 3(a) presents the evolution of the pulse of medium height under the sweep of detuning  $\delta$  from its negative to positive values. As it has been shown above, when the Lorentz field effect is weak ( $\alpha < 1$ ), the step pulse suffers a strong coherent interaction with the layer accompanying by the formation of sharp spikes of superradiation [Fig. 3(b)] with a remarkable satellite spike in the later time moments [17].

The reason for the decline and the subsequent growth of  $T_{tr}$  vs  $\delta$  in Fig. 3(c) is the change of resonance conditions of field interaction with layer, while a sudden narrow maximum in the bottom of the cited plot is the result of the blooming of resonance film by intensive peaks of radiation on the contour of transmitted field [see Figs. 1(c) and 2(c)].

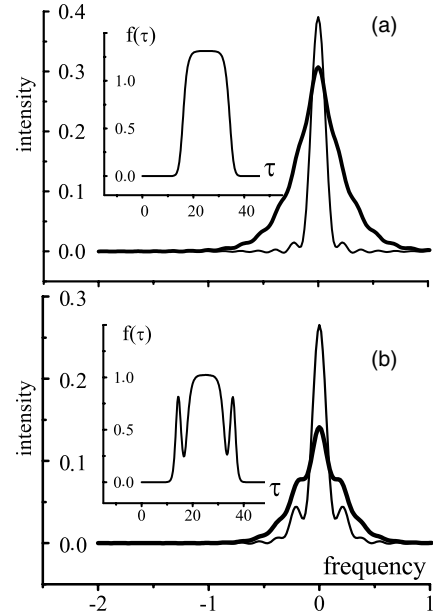


FIG. 5. The spectra of the incident (thin solid curve) and transmitted pulses (thick solid curve) corresponded to: (a) Figs. 3(d)–3(f) and (b) Figs. 4(d)–4(f). In the insets  $f(\tau)$  is the field penetrating the film (see the text) for (a)  $T_1=0$ ,  $T_2=0$  and (b)  $T_1=2$ ,  $T_2=-4$ . All variables are dimensionless.

A microscopic Lorentz field introduces an additional dynamic contribution to the total detuning  $\delta_{tot}(\tau)=\delta+an(\tau)$ , which is proportional to the resonance level population difference. In consequence, the process of strong coherent interaction of radiation with atomic ensemble starts earlier at negative detuning and the region of coherent interaction becomes wider in  $\delta$  domain [Fig. 3(d)]. The number of spikes also increases [Fig. 3(d)] as new peaks appear every time the total detuning changes its sign [these moments are marked by two spots in Fig. 3(e)]. The enhancement of a local field effect contribution apparently leads to the distortion of the transmission coefficient  $T_{tr}$  spectrum. There is a slight shift to the negative side and the broadening of the above quoted maximum [Fig. 3(f)].

### D. The effect of substrate dispersion

The effect of substrate material dispersion strongly depends on the value and the sign of the dispersion coefficients  $T_1$  and  $T_2$ , leading to a form distortion [Figs. 4(a), 4(b), 4(e), and 4(f)] and spectrum changing [Fig. 5]. The numerical simulation in this paragraph exhibits one certain realization of a dispersion effect from a set of possibilities.

In Fig. 4, which is analogous to Fig. 3, the effect of substrate dispersion is presented for two cases when the local field effect is off ( $\alpha=0$ ) [Figs. 4(a)–4(c)] and when it is on ( $\alpha=1$ ) [Figs. 4(d)–4(f)].

The region of resonance, where we drag the quantum system in by sweeping the detuning  $\delta$ , is getting wider due to the change of spectrum of the refracted field. The coherent interaction of field with the film manifests in a sharp spike of transmitted radiation [Fig. 4(c)] in the vicinity of resonance.

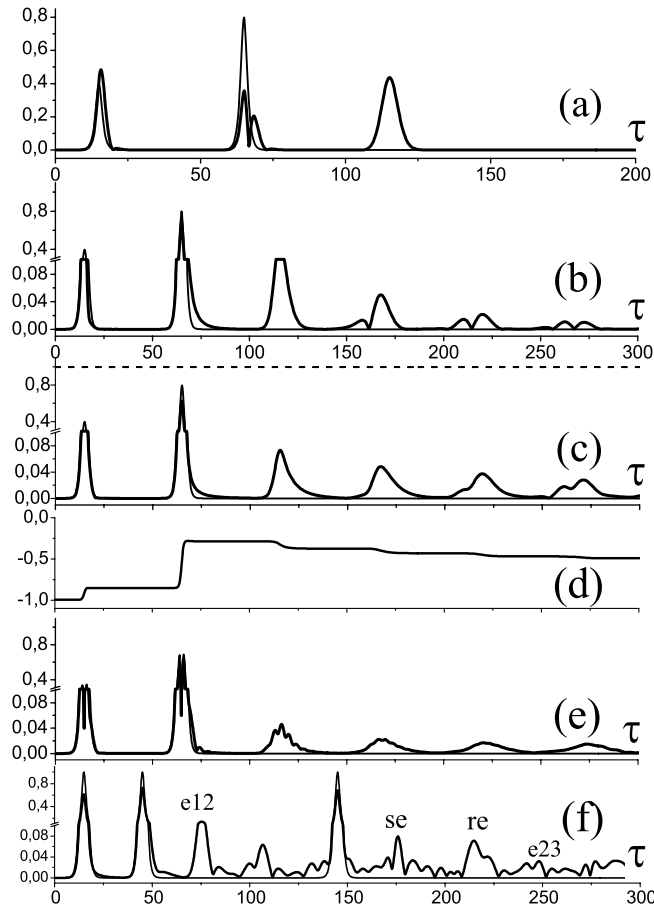


FIG. 6. The photon echo effect in a thin layer of resonance atoms. (a) Refracted wave  $f(\tau)$  (thin solid curve), polarization of film  $\langle\sigma_v\rangle$  (thick solid curve),  $\alpha=0$ ,  $g=0$ ; (b) multiple photon echo, transmitted wave  $|e_{tr}(\tau)|$  (thick solid curve), incident wave  $e_{in}(\tau)$  (thin solid curve),  $\alpha=0$ ,  $g=0.15$ ; (c) multiple photon echo, Bloch vector length  $|\langle\sigma_v\rangle|^2 + n_v^2$  (dashed line),  $\alpha=0.6$ ,  $g=0.15$ ; (d) inversion  $\langle n_v \rangle$ ; (e) photon echo in the presence of substrate dispersion  $T_1=0.7$ ,  $T_2=-0.7$ ; (f) three pulse echo. All variables are dimensionless.

The layer on a dispersive substrate becomes dark in the transmitted light [Fig. 4(b)]. With the including of local field effect [Figs. 4(d)–4(f)] the population difference provides the dynamical contribution to a total detuning  $\delta_{tot}$ , making it the time depending value [Fig. 4(f)] and provoking a spectrum distortion (Fig. 5). Consequently the temporal profile of a transmitted field gets more complex in the region of effective coherent interaction [Figs. 4(e) and 4(f)].

#### IV. PHOTON ECHO IN A THIN FILM OF RESONANCE ATOMS

The photon echo [41] is a coherent response of an ensemble of quantum resonance systems (two or more level atom) to a series of ultrashort pulses. Photon echo arises at the moments multiple to time intervals between pulses as the result of phase synchronization of individual radiators with detuning  $\nu$  comprising the inhomogeneous line. The latter process is represented by the averaging  $\langle \dots \rangle$  in the set of

basic equations (11). The difficulty in solving (11) is that the field which acts on atom  $e_{loc}(\tau)$  in its turn does depend on averaged polarizability  $\langle\sigma_v\rangle$ , that makes the problem self-consistent.

So far there have been several approaches to resolve the problem by admitting the simplifying suggestions [25,28,30]. We report the results of one more attempt to tackle the problem in full including local field effect, inhomogeneous broadening, and dispersion of substrate. Equations (11) were solved with the desired accuracy by iterations over field, which started from the field entering the film. The length of the Bloch vector was monitored at every iteration step and at every point of time grid.

In Fig. 6(a) effect of photon echo is depicted with parameter  $g$  formally equals to zero. That corresponds to an approximation of given field. The signal of primary echo is detected in polarization, so the field of a reciprocal reaction of resonance medium is negligible. The picture of multiple echo in Fig. 6(b), where  $g \neq 0$ , (echo from echo) is typical for coherent effects in optically dense medium [45].

The local field effect [Fig. 6(c)] causes dynamical shifts of spectral components inside the inhomogeneous line, thus leading to a general smoothing of the time shape of coherent responses. Note that the length of Bloch vector averaged over the spectral line keeps constant [Fig. 6(c) dashed line].

Additional spectral broadening due to substrate dispersion [Fig. 6(e)] acts in the same direction thus depleting the chain of multiple photon echoes. It should be emphasized, that the population difference changes significantly during the excitation and echo formation, as it is shown in Fig. 6(d). Figure 6(f) demonstrates the effect of three-pulse excitation attributed by generation of stimulated echo (se) in the appropriate moment, as well as reconstructed echo (re) [42], and echoes from the pairs of external pulses. This is a unique result in thin layer optics accounting the local field effect. The substrate dispersion effect for stimulated echo is trivially similar to that in Fig. 6(e).

#### V. CONCLUSION

In conclusion, the numerical analysis of coherent responses of resonance thin film to ultrashort optical pulse excitation is presented. The role of inhomogeneous broadening of resonance line, the local field effect, and the substrate dispersion was demonstrated in both the temporal shape of transmitted wave and the integral transmission coefficient. There is a range of incoming amplitudes where the interaction of pulsed light with the quantum system leads to the formation of peaks of superradiation in a transmitted wave. Photon echo effect is considered without conventional simplification. It turns out that a film of resonance atoms is able to radiate multiple echo signals after the irradiation by two or more coherent pulses.

#### ACKNOWLEDGMENTS

The author gratefully acknowledges fruitful discussions with Andrei I. Maimistov and Askhat M. Basharov. The research is supported by the RFBR Grant No. 06-02-16406.

- [1] A. I. Maimistov and A. M. Basharov, *Nonlinear Optical Waves* (Kluwer, Dordrecht, 1999).
- [2] J. J. Hopfield, Phys. Rev. **112**, 1555 (1958).
- [3] V. M. Agranovich, Sov. Phys. JETP **37**, 307 (1960).
- [4] L. C. Andreani, in *Confined Electrons and Photons*, edited by E. Burstein and C. Weisbuch (Plenum, New York, 1995), p. 57.
- [5] L. C. Andreani, F. Tassone, and F. Bassani, Solid State Commun. **77**, 641 (1991).
- [6] D. S. Citrin, Phys. Rev. B **49**, 1943 (1994).
- [7] G. Panzarini and L. C. Andreani, Solid State Commun. **102**, 505 (1997).
- [8] V. M. Agranovich, V. Y. Chernyak, and V. I. Rupasov, Opt. Commun. **37**, 363 (1981).
- [9] T. Shimooka, S. Yoshimoto, M. Wakisaka, J. Inukai, and K. Itaya, Langmuir **17**, 6380 (2001).
- [10] V. M. Agranovich and M. D. Galanin, *Electron Excitation Energy Transfer in Condensed Matter* (Nauka, Moskva, 1978).
- [11] F. Tassone, C. Piermarocchi, V. Savona, A. Quattropani, and P. Schwendimann, Phys. Rev. B **56**, 7554 (1997).
- [12] F. Tassone and Y. Yamamoto, Phys. Rev. B **59**, 10830 (1999).
- [13] G. Khitrova, H. M. Gibbs, F. Jahnke, M. Kira, and S. W. Koch, Rev. Mod. Phys. **71**, 1591 (1999).
- [14] L. Allen, J. H. Eberly, *Optical Resonance and Two-Level Atoms* (Wiley, New York, 1975).
- [15] V. M. Agranovich, V. I. Rupasov, and V. Y. Chernyak, Fiz. Tverd. Tela (Leningrad) **24**, 2992 (1982).
- [16] H. E. Ponath and M. Schubert, Opt. Acta **30**, 1139 (1983).
- [17] E. Vanagas and A. I. Maimistov, Opt. Spectrosc. **84**, 258 (1998).
- [18] E. Vanagas, Lith. Phys. J. **32**, 330 (1992).
- [19] E. Vanagas, Lith. Phys. J. **32**, 416 (1992).
- [20] X. Zhu, M. S. Hybertsen, P. B. Littlewood, and M. C. Nuss, Phys. Rev. B **50**, 11915 (1994).
- [21] H. Glaeske, V. A. Malyshev, and K.-H. Feller, J. Chem. Phys. **114**, 1966 (2001).
- [22] H. A. Lorentz, *The Theory of Electrons* (Dover, New York, 1952).
- [23] M. E. Crenshaw and C. M. Bowden, Phys. Rev. A **53**, 1139 (1996).
- [24] M. G. Benedict, V. A. Malyshev, E. D. Trifonov, and A. I. Zaitsev, Phys. Rev. A **43**, 3845 (1991).
- [25] M. G. Benedict and E. D. Trifonov, Phys. Rev. A **38**, 2854 (1988).
- [26] P. I. Khadji and S. L. Gaivan, IEEE J. Quantum Electron. **27**, 532 (1997).
- [27] V. I. Rupasov and V. I. Yudson, Sov. J. Quantum Electron. **12**, 1415 (1982).
- [28] S. M. Zakharov and E. A. Manykin, JETP **78**, 566 (1994).
- [29] S. M. Zakharov and E. A. Manykin, Opt. Spectrosc. **63**, 1069 (1987).
- [30] V. A. Goryachev and S. M. Zakharov, Kvantovaya Elektron. (Moscow) **24**, 251 (1997).
- [31] Y. Ben-Aryeh, C. M. Bowden, and J. C. Englund, Phys. Rev. A **34**, 3917 (1986).
- [32] A. M. Basharov, Sov. Phys. JETP **67**, 1741 (1988).
- [33] Yu. A. Logvin, A. M. Samson, and S. I. Turovets, Sov. J. Quantum Electron. **20**, 1425 (1990).
- [34] A. M. Basharov, JETP **81**, 459 (1995).
- [35] Y.-K. Yoon, R. S. Bennink, R. W. Boyd, and J. E. Sipe, Opt. Commun. **179**, 577 (2000).
- [36] S. O. Elyutin, A. I. Maimistov, Proc. SPIE **4605**, 171 (2001).
- [37] S. O. Elyutin and A. I. Maimistov, Opt. Spectrosc. **84**, 258 (1998).
- [38] V. A. Malyshev, F. Carreno, M. A. Anton, O. G. Calderon, and F. Dominiguez-Adame, J. Opt. B: Quantum Semiclassical Opt. **5**, 313 (2003).
- [39] A. M. Basharov, A. I. Maimistov, and S. O. Elyutin, JETP **88**, 16 (1999).
- [40] S. O. Elyutin and A. I. Maimistov, J. Mod. Opt. **46**, 1801 (1999).
- [41] D. Abella, N. A. Kurnit, and S. R. Hartmann, Phys. Rev. **141**, 391 (1966).
- [42] E. A. Manykin and V. V. Samartsev, *Optical Echo-Spectroscopy* (Nauka, Moskva, 1984).
- [43] S. Özçelik and D. L. Akins, Appl. Phys. Lett. **71**, 3057 (1997).
- [44] S. L. McCall and E. L. Hahn, Phys. Rev. **183**, 457 (1969).
- [45] S. O. Elyutin and A. I. Maimistov, JETP **93**, 737 (2001).